PERGAMON

Vision Research 41 (2001) 1901–1914

Vision Research

www.elsevier.com/locate/visres

Broad direction bandwidths for complex motion mechanisms

T.S. Meese [a,*], M.G. Harris [b]

[a] *Neurosciences Research Institute, Aston University, Aston Triangle, Birmingham, B4 7ET, UK*
[b] *School of Psychology, University of Birmingham, Edgbaston, Birmingham, B15 2TT, UK*

Received 11 July 2000; received in revised form 8 February 2001

Abstract

Growing evidence from psychophysics and single-unit recordings suggests specialised mechanisms in the primate visual system for the detection of complex motion patterns such as expansion and rotation. Here we used a subthreshold summation technique to determine the direction tuning functions of the detecting mechanisms. We measured thresholds for discriminating noise and signal + noise for pairs of superimposed complex motion patterns (signal A and B) carried by random-dot stimuli in a circular 5° field. For expansion, rotation, deformation and translation we found broad tuning functions approximated by $\cos(d)$, where d is the difference in dot directions for signal A and B. These data were well described by models in which either: (a) cardinal mechanisms had direction bandwidths (half-widths) of around 60°; or (b) the number of mechanisms was increased and their half-width was reduced to about 40°. When $d = 180°$ we found summation to be greater than probability summation for expansion, rotation and translation, consistent with the idea that mechanisms for these stimuli are constructed from subunits responsive to relative motion. For deformation, however, we found sensitivity declined when $d = 180°$, suggesting antagonistic input from directional subunits in the deformation mechanism. This is a necessary property for a mechanism whose job is to extract the deformation component from the optic flow field.

Keywords: Subthreshold summation; Expansion; Deformation rotation; Optic flow; Inhibition

1. Introduction

Following early work by Regan and Beverley (1978), psychophysical evidence emerged during the 1990s for pooling mechanisms equipped for detecting complex patterns of motion such as expansion, rotation and deformation (e.g. Morrone, Burr, & Vaina, 1995; Harris & Meese, 1996; Gurney & Wright, 1996; see Bex, Metha, & Makous, 1999 for a recent review). As happened in spatial vision (Graham, 1989), the discovery of these mechanisms prompted a programme of exploration and characterisation. For example, Burr, Morrone, and Vaina (1998) used random dot patterns (DeBruyn & Orban, 1990; Edwards & Badcock, 1993) and a spatial summation technique (Morrone et al., 1995) to investigate the size of their receptive fields. They concluded that they were as large as 72°, though whether additional smaller mechanisms also exist is not known. Evidence does suggest, however, that different mechanisms do exist for different patterns of complex motion. For example, Meese and Harris (under review) plotted psychometric functions for orthogonal patterns of rotation and expansion, and for orthogonal configurations of deformation. They found a small amount of summation consistent with probability summation, implying that observers used multiple complex motion mechanisms in parallel (or rapid serial) to detect the stimuli.

The sampling density of mechanisms for one class of complex motion patterns was addressed by Morrone, Burr, and DiPietro (1999). These authors collapsed data across a group of observers and found sensitivity for radiating[1] and rotating stimuli to be greater than

* Corresponding author. Tel.: +44-121-3593611, ext. 5421; fax: +44-121-3334220.
E-mail addresses: t.s.meese@aston.ac.uk (T.S. Meese), m.w.harris@bham.ac.uk (M.G. Harris).

[1] Some authors have chosen to use speed gradients in their stimuli while others have kept speed constant across the entire display. While the terminology used to describe rotating stimuli does not distinguish between the two, the terms 'expansion' and 'contraction' are typically used for appropriate stimuli that contain speed gradients whereas the term 'radiation' is often used for similar stimuli containing no speed gradient.

0042-6989/01/$ - see front matter
PII: S0042-6989(01)00083-9

that for intermediate spiralling patterns. They accounted for this by supposing that performance was mediated by cardinal mechanisms (for radiation and rotation) with broad direction tuning (bandwidths of $\pm 60°$). However, these results do not rule out the possible existence of spiral selective mechanisms. For example, as Morrone et al. point out, it could be that spiral mechanisms have lower sensitivity than radiation and rotation mechanisms and so were not revealed by their experiment. Indeed, Snowden and Milne (1996) have argued for the existence of these mechanisms. They measured threshold elevation for complex motion after adapting to expansion, rotation and spirals and were unable to describe their results using only cardinal mechanisms. A model incorporating multiple mechanisms, including those sensitive to spirals, with direction bandwidths of $\pm 47°$ (half-width at half-height) was consistent with their results.

In sum, although sampling density of complex motion mechanisms remains unclear, current evidence does suggest that the mechanisms are broadly tuned. In the present paper we use a subthreshold summation technique to investigate further the stimulus selectivities of the detecting mechanisms for translating, expanding, rotating, and deforming random dot stimuli. While previous studies have addressed the question of bandwidth (as outlined above), none has used a summation technique nor such a broad range of stimulus patterns. Furthermore, as outlined below, the direction bandwidth of complex motion mechanisms is of particular theoretical importance.

1.1. Mechanism bandwidths for complex motion: theoretical implications

Consider the following two possibilities. At one extreme, complex motion mechanisms might be selective for specific instances of complex motion. For example, a mechanism from this class might respond to little other than a purely rotating textured stimulus in the fronto-parallel plane. At the other extreme, a mechanism might extract from a complex motion field the vector component to which it is tuned. For example, a rotation mechanism might give the same response to a rotating stimulus regardless of whether it is vector summed with components of expansion, deformation and translation. In the first case, the tight stimulus selectivity would require narrow direction bandwidths. In the second case, the mechanism, which we refer to as a *complex motion extractor*, would need several properties as outlined by Zhang, Sereno, and Sereno (1993). These are: (i) cosine direction tuning functions; (ii) inhibitory input in the antipreferred direction (specifically, the subunits should have direction tuning that is cosine over $\pm 180°$); (iii) a direction template matched to the mechanism's preferred stimulus; (iv) subunits that respond linearly to speed; and (v) subunits whose weight is proportional to the local vector length in the vector field of the preferred stimulus. In Experiment 1 we found evidence for the first property, though we also show that the results are consistent with narrower bandwidths if the sampling density of detecting mechanisms is increased. In Experiment 2 we found evidence for the second property for deformation but not expansion, rotation or translation. This result for deformation is confirmed in Experiment 3. There is some discussion of the third property below. We do not address the fourth or fifth properties.

1.2. Direction templates for complex motion

Here we clarify some of our terminology and consider various possible direction templates for the complex motion mechanisms investigated in this paper. By complex motion mechanism we refer to the mechanism (or set of mechanisms) that is used by vision to detect a particular pattern of complex motion. So, for example, the most obvious type of expansion mechanism is something whose receptive field has a directional template that resembles an expanding pattern. We describe such a mechanism as *two-dimensional* because two (orthogonal) axes are required to describe its direction template. In contrast, by *one-dimensional* mechanism we mean a detecting mechanism whose direction template varies along only a single axis. In this case, different regions of the template might be responsive to *opposite* directions of motion. For example, a one-dimensional shear mechanism might be responsive to rightward motion in the upper part of its receptive field and leftward motion in the lower part of its receptive field. In principle, complex motion mechanisms could consist of pairs of appropriate and orthogonal one-dimensional mechanisms (Meese & Harris, 1997). Indeed, simulations of observer movement about artificial environments suggest that for deformation, such mechanisms might be more appropriate (Ivins, Porrill, Frisby, & Orban, 1999).

Two-dimensional mechanisms, and the type of one-dimensional mechanism discussed here, both fall within a class of complex motion mechanisms that pool over position and direction; for the two-dimensional mechanism, the number of directions could be many, but for the one-dimensional mechanism, the maximum number of directions is two. Summation studies (Morrone et al., 1995; Harris & Meese, 1996; Burr et al., 1998; Meese & Harris, under review) indicate that complex motion mechanisms pool across different directions at different regions in the stimulus, but in some cases it is not yet clear whether the mechanisms involved are one-dimen-

sional, two-dimensional or both. We note, however, that in previous work (Meese & Harris, under review), as well as for observers who performed appropriate conditions in the present paper (TSM and CHD), sensitivity to deformation is slightly less than it is to rotation and expansion. Assuming that complex motion mechanisms have equal gain, this would be expected if deformation were detected by an orthogonal pair of one-dimensional shear mechanisms but rotation and expansion were detected by more efficient two-dimensional mechanisms with direction templates matched to their preferred stimuli. It is important to note, however, that whether the detecting mechanisms are one- or two-dimensional has no bearing on the model predictions presented in this paper. We explain why this is so in Appendix C.

2. Methods

2.1. Equipment, stimuli and task

Stimuli were displayed on a 120 Hz monitor using the framestore of a VSG2/3 stimulus generator under the control of a PC. A 2IFC paradigm was used to measure the detection thresholds (sometimes called coherence thresholds) of complex motion in random dot stimuli where the observer's task was to discriminate signal + noise from noise alone (Snowden & Milne, 1996). Responses were made by pressing one of two buttons[2] to indicate the interval thought to contain the signal. Correctness of response was indicated using auditory feedback. Observers were familiar with the stimuli, and experimental sessions began with high signal levels to remind observers of their appearance.

For each test interval, up to 440 bright dots were presented on a dark background with their nominal positions randomised from trial to trial. Dot luminance was modulated by an annular window with inner and outer diameters (zero contrast) of 0.2 and 5.5°. Linear ramps at the inner and outer boundaries of the window were 0.7° wide, giving a full-height plateau-width of 1.25°. The general impression of the stimulus was of a circular display with a diameter of about 5°, with a small hole in the centre. Both temporal intervals contained a movie consisting of four sequential images (Morrone et al., 1995) each of which was displayed for nine frames. This produced stimuli that appeared to move smoothly and had a duration of 300 ms.

[2] In general, we use a procedure where the response is triggered by the offset of a button press which is recorded only if the other button is not depressed simultaneously. This procedure has the advantage that a sophisticated observer is often able to correct finger errors (pressing the 'wrong' button by mistake) by depressing the 'correct' button before releasing the 'wrong' button, and then finally releasing the 'correct' button.

A dot's nominal polar angle ($\theta°$) is given by $\arctan(y/x)$, where (x, y) are its Cartesian coordinates half way through its trajectory and the origin is in the centre of the display. Thus, the motion directions of signal dots are given by: $(\theta)°$, $(\theta - 90)°$, $(90 - \theta)°$ for expansion, clockwise rotation and deformation, respectively. Noise dots had random directions allocated independently on each trial, but were otherwise identical to the signal dots. Furthermore, noise dots in the signal + noise interval were matched to noise dots in the noise interval. In other words, the only difference between the two stimulus intervals was the presence of signal dots in the signal + noise interval which replaced some of the noise dots contained in the noise alone interval.

In complex motion stimuli, each dot travelled linearly through 10% of its nominal distance (D) from the origin, where $D = \sqrt{(x^2 + y^2)}$. Thus, our stimuli contained global speed gradients, though individual dots had constant velocity. This arrangement ensured that on average, all complex motion stimuli had the same distribution of dot velocities (i.e. all stimuli contained the same speed gradient and had dot directions evenly distributed around 360°), allowing meaningful comparisons to be made between conditions. The maximum dot speed was 0.92° s^{-1} at the very outer edge of the stimulus where dot luminance was at its dimmest.

For a translation condition, signal dots all travelled in the same direction and noise dots travelled the same distance but each in a different random direction. Translation stimuli contained no speed gradients and for observer CHD the dots travelled a distance of 0.125° (speed = 0.42° s^{-1}). This is the same distance as that travelled by a dot in a complex motion pattern positioned halfway between the centre and the edge of the nominal 5° display region. For observer NH, dots travelled more slowly covering a distance of 0.089° (speed = 0.30° s^{-1}).

For all stimuli the algorithm of Georgeson, Freeman, and Scott-Samuel, (1996) was used to achieve sub-pixel accuracy. In brief, this technique uses a set of four pixels arranged in a square to represent a single dot. The luminance levels of these pixels are manipulated in a systematic way to control the location of their centroid which corresponds to the perceived location of the dot (Morgan & Aiba, 1985; Georgeson et al., 1996).

2.2. Procedure and observers

A three-down, one-up staircase procedure (Wetherill & Levitt, 1965; Meese, 1995) controlled, in log steps, the proportion of signal dots (i.e. the proportion of dots whose directions were not randomised) contained in the stimulus. For each stimulus, data were collapsed from a pair of interleaved staircases (Cornsweet, 1962), each of which terminated after eight staircase reversals (i.e. 16 reversals for each stimulus). This procedure

produced a data set for each estimation of threshold of about 100 trials. Thresholds were measured for discriminating 'signal + noise' from 'noise alone' using probit analysis (Finney, 1971) and expressed as percentage of signal dots (S) in the stimulus at the 75% correct point. To try to reduce variability, the data were discarded and the experimental session was re-run if the standard error of any of the estimates of threshold performed by probit analysis (McKee, Klein, & Teller, 1985) was greater than 0.15 log units.

Experimental sessions began with a staircase procedure to measure psychometric functions for each of two complex motion signals referred to as signal A and B (Fig. 1). The observer was then given an auditory indication that the stimuli were to be changed, and the next stage of the experiment, in which the psychometric function for a compound stimulus was measured, was started by the observer pressing a button. The relative contributions of the two signals in the compound were determined by the thresholds for the two signals (S_A, S_B) when presented in isolation in the first stage. Specifically, weights for the two signals (wt_A, wt_B) were given by: $wt_A = S_A/(S_A + S_B)$ and $wt_B = S_B/(S_A + S_B)$. This method aimed to produce compound stimuli containing stimulus components to which the observer was similarly sensitive.

Summation was measured for pairs of motion stimuli (signal A and B) using each of the four different stimulus configurations illustrated schematically in Fig. 1. In each series of conditions, the configuration of signal A was fixed (e.g. vertical translation in Fig. 1A). Signal B was similar to signal A, but had the local directions of its dot trajectories rotated by angle d, where $d = 15, 30, 45, 60, 75$ and $90°$. Thus, if signal A was expansion (Fig. 1B) and $d = 90°$, then signal B was rotation. Note that for convenience we report the absolute value of d, though for the stimuli in Fig. 1C, signal B dots were rotated in the opposite directions to those in the other conditions. In the translation condition, signal A translated vertically for NH (as

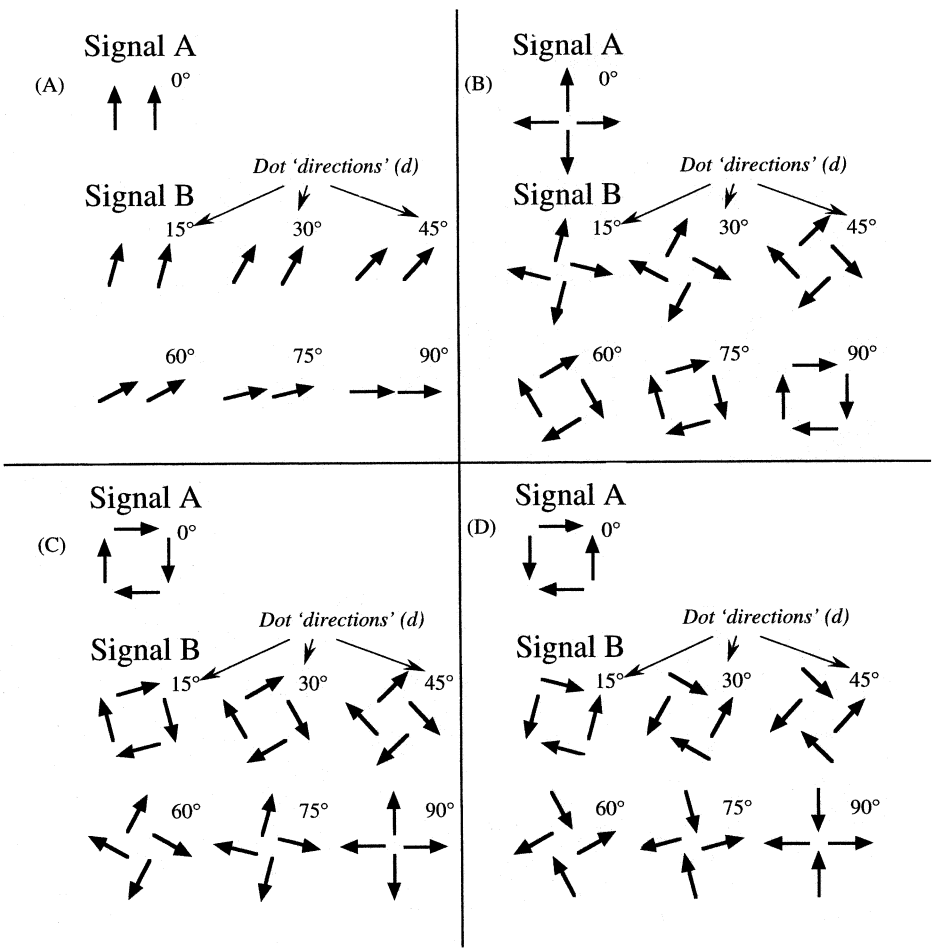

Fig. 1. Schematic illustration of stimulus conditions used in Experiment 1. Signal A was translation (A), expansion (B), rotation (C) and deformation (D). Signal B was similar to signal A, but had the direction of each dot trajectory rotated by $d°$. Note that for convenience, d is reported without sign.

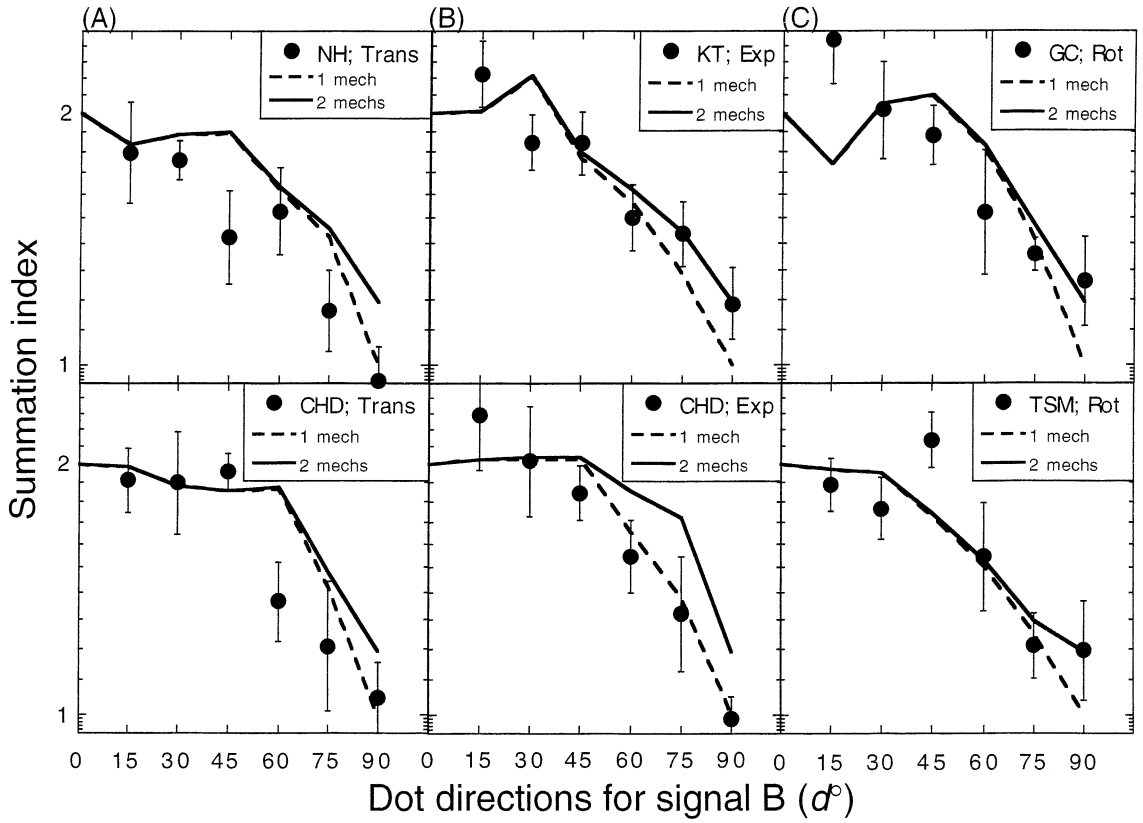

Fig. 2. Summation index ($SI = S_A/S_{A(cmpnd)}$) on a log scale as a function of the dot directions for signal B (d_B in Appendix A). Results are shown for two observers when signal A was translation (A), expansion (B) and rotation (C). Data points are geometric means and error bars show ± 1 SE. The model curves are for mechanisms with smooth cosine direction tuning. Note, however, that the predictions are kinked because of the different empirical estimates of mechanism gain at different positions along the function. (See text and Appendix A for details.)

shown in Fig. 1) and horizontally (from left to right) for CHD. For each stimulus type (e.g. Fig. 1A), different stimulus conditions (different values of d) were performed in randomised blocks and data were averaged from at least six blocks.

Observers were the authors (TSM, MGH) and four undergraduate students at Aston University (NH, KT, GC and CHD), three of whom completed the experimentation as part of their undergraduate project work. All observers had normal or corrected to normal vision.

2.3. Control experiment

In an initial control experiment we measured sensitivity to 300 ms presentations of only the final image of the movie sequences where 25% of the total number of dots were designated signal dots. Performance was around chance (50% correct), indicating that potential position or dot density cues were not available to observers. In order to be able to detect the signal in the moving stimuli investigated in this paper, observers must have integrated stimulus information over a series of image frames.

3. Results and discussion

3.1. Experiment 1: broadly tuned summation suggests broadly tuned mechanisms for complex motion

Summation indices (SI) were calculated for each signal pair as follows: $SI = S_A/S_{A(cmpnd)}$, where S_A and $S_{A(cmpnd)}$ are the thresholds for signal A when presented alone (with noise) and when contained in the compound stimulus, respectively (Watson, 1982). Fig. 2 shows SI as a function of d for translation, expansion and rotation, and Fig. 3 is for deformation (note the log scale for SI in both figures). For all stimuli and all observers, summation is very broadly tuned suggesting broad bandwidths for the detecting mechanisms. The two curves are for the models described in Appendix A which contain mechanisms with direction bandwidths given by $\cos(d)$. The dashed curve is for a parameterless model which includes a single mechanism selective for signal A. The solid curve is for a similar model but which contains an additional mechanism selective for signal B with $d = 90°$. In this model, the two mechanisms are summed using the Quick pooling formula (Quick, 1974) with an exponent of four which is widely

used to represent probability summation (Graham, 1989; Meese & Williams, 2000). In all cases, the models provide a fair account of the data, though there is a tendency for the data to fall slightly below the predictions, indicating that the bandwidth for summation is slightly more narrowly tuned than a cosine function. We address the question of assessing direction bandwidth of the detecting mechanisms more closely in the next subsection.

Note that when $d = 90°$, the data typically fall between an SI of 1.19 (solid curve) and an SI of 1 (dashed curve). These extremes are consistent with: (i) probability summation between two independent detecting mechanisms; and (ii) a strategy in which only a single mechanism is monitored at any one time. Both of these extremes have been reported previously for different data but similar stimulus conditions (Meese and Harris, under review).

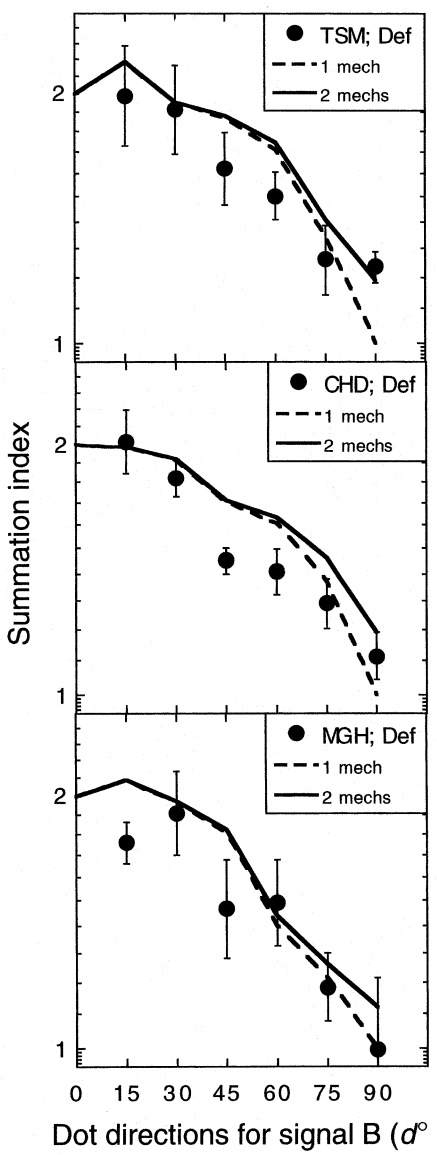

Fig. 3. As Fig. 2, but signal A was deformation and results are shown for three observers. The results are very similar to those for the other stimulus conditions in Fig. 2.

3.2. Mechanism bandwidth

The results from Experiment 1 are well described by a model in which complex motion mechanisms have broad (cosine) direction bandwidths. This is consistent with the first of the properties required for a complex motion extractor as outlined in the introduction (Zhang et al., 1993). The model predictions in Figs. 2 and 3 are for mechanisms tuned for cardinal directions, but there are several other models that should be considered.

In the analysis that follows we assume that probability summation occurs amongst all mechanisms and that the proportion of signal dots in signal A and B is such that each signal is equally detectable when presented alone (see Appendix B for further details). In general, to fit the new models to the data would require that the gains of the detecting mechanisms be free parameters. Indeed, that gain might vary across mechanisms was one reason for employing the signal normalisation procedure in the experiments. Furthermore, because signal normalisation was performed independently for each condition of signal B, the data would not generally constrain the fits. Instead, we settle for making the simplifying assumption that gain is the same for all mechanisms. This allows the effects of bandwidth and number of mechanisms to be compared directly across models.

In Fig. 4A, mechanisms have cosine bandwidths and four predictions are shown. Two of these (the solid curve and the medium dashed curve beneath it) employ the same mechanisms as the models plotted in Figs. 2 and 3. Thus, these earlier models which provided a reasonable fit to the data, can be compared with the new models. Note that in all cases, mechanisms are evenly spaced on the dimension d (for example, for the solid curves, the spacing between mechanisms is 90°) and that in Fig. 4 the total number of evenly placed mechanisms is reported rather than the number of stimulated mechanisms as was the case in Figs. 2 and 3.

The curve labelled '4 intermediate mechanisms' in Fig. 4A shows the effect of rotating the mechanism axes by 45° relative to signal A. So, for example, when signal A is rotation or expansion (Fig. 1B, C), the preferred stimuli of the four detecting mechanisms are four different spiral patterns (expanding clockwise; expanding anticlockwise; contracting clockwise; contracting anticlockwise). This rotation of axes causes the model to predict far too much summation: for half of the function it is well above the solid curve which tended to lie on or above the data in Figs. 2 and 3. By including a total of eight mechanisms (four cardinal plus four intermediate; dotted curve), summation is reduced but

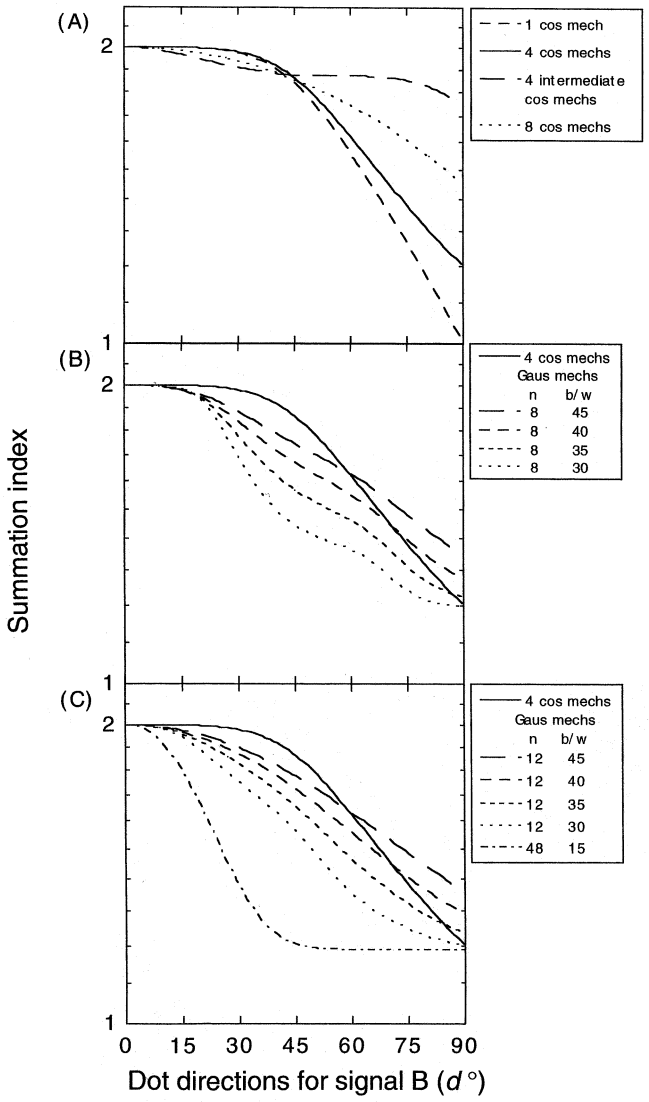

Fig. 4. Model predictions assuming: mechanisms with equal gain, normalised levels of signal dots in signal A and B and probability summation between all mechanisms. In all cases, model mechanisms are placed so as to correspond with even intervals of *d*. (A) Mechanisms all have cosine direction tuning. Different curves are for different numbers of mechanisms and different positions relative to cardinal axes; (B) The solid curve is the same as that in (A). Other curves are for a model containing eight mechanisms with Gaussian direction tuning functions of various bandwidths. Half-widths at half-height are indicated in the insets in degrees; (C) The solid curve is the same as that in (A) and (B). Other curves are for models containing either 12 or 48 mechanisms with Gaussian direction tuning functions and various bandwidths. (See text and Appendix B for model details.)

is still greater than that for the four cardinal mechanisms. Thus, as the minimum number of mechanisms that it is reasonable to consider is four (e.g. Morrone et al., 1999), we note that for such a model to account for the present data, the mechanisms must be aligned with the cardinal axes and have broad (cosine) direction tuning.

Notwithstanding the remarks above, Figs 4B–C show that other plausible models do exist. In these figures the solid curves show the model with cardinal mechanisms and cosine bandwidths as before, and is included for purposes of comparison. The dashed curves show that similar amounts of summation can be achieved by decreasing the bandwidth and increasing the number of mechanisms (Graham, 1989). Fig. 4B shows four examples for eight mechanisms (spaced at intervals of 45°), with half-widths of 30, 35, 40 and 45° and Fig. 4C shows the same four bandwidths for 12 mechanisms (spaced at intervals of 30°). For both numbers of mechanisms there are curves that fall close or just below the solid curve, suggesting that these are plausible candidates for the data in Figs. 2 and 3. The extent to which bandwidth and number of mechanisms can be traded off against each other is limited however: the fourth curve in Fig. 4C (fine dashes) is for 48 mechanisms (spaced at intervals of 7.5°) with half-widths of 15°. This model falls very much below the solid curve and consequently much underestimates the amount of summation seen in the data. As matters are not improved by increasing the number of mechanisms the bandwidths of complex motion mechanisms cannot be this narrow. Thus, our data are not consistent with one idea outlined in Section 1, that vision contains complex motion mechanisms that are tuned to specific instances of complex motion. In sum, our data suggest either: (a) four very broadly tuned (half-width $\approx 60°$) cardinal mechanisms; or (b) a larger number (e.g. eight) of less broadly tuned mechanisms (e.g. half-width $\approx$ 40°).

3.3. Experiment 2: summation and antagonism for opposite motion directions

The data for Experiment 2 were gathered contemporaneously with those for Experiment 1. In this experiment, dots in signal B travelled in opposite directions to those in signal A (i.e. $d = 180°$) to test for the second property of complex motion extractors: that they receive inhibitory input in the antipreferred direction. Summation indices are plotted in Fig. 5, and are for different observers and different stimulus patterns used for signal A (translation, expansion, rotation, deformation). The horizontal dashed line shows a prediction for probability summation between two independent detecting mechanisms. For most observers, the amount of summation is greater than this when signal A was translation, expansion or rotation. It remains unclear to us how best to interpret this result, but one possibility is that unidirectional motion mechanisms feed into higher order complex motion mechanisms (Freeman & Harris, 1992; Sekuler, 1992; Morrone et al., 1995; Gurney & Wright, 1996; Bex, Metha, & Makous, 1998), and that the unidirectional mechanisms respond to

relative motion rather than absolute motion. One way in which this could be achieved is for these mechanisms to have a surround region that responds constructively to motion in the opposite direction to the mechanism's preferred direction in its centre (Allman, Miezin, & McGuiness, 1985). This issue clearly requires further attention.

A second striking feature of Fig. 5 is that when signal A was deformation, the compound stimulus was more difficult to detect than either of the components presented in isolation (i.e. the SI < 0). Previously we have reported that coherence thresholds for deformation are often a little higher than for other motion stimuli (Meese & Harris, under review) and we wondered whether this might be in some way linked to the present results. For example, one possibility is that the deficit in performance was due to antagonism within local motion mechanisms and that this manifested itself only at high signal levels. Fig. 6 shows the coherence thresholds for the component signals in Experiment 2. There is no clear relation between the pattern of results in Fig. 6 and that in Fig. 5, suggesting that the number of signal dots contained in the stimuli was not a crucial factor for the pattern of results in Fig. 5.

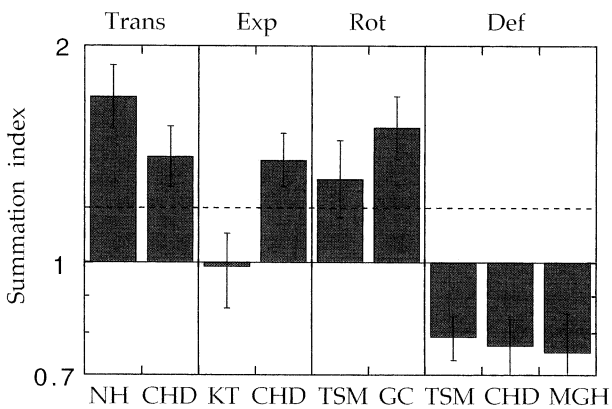

Fig. 5. Summation indices from Experiment 2. Results are for several observers where signal A was the same as that shown in Fig. 1 and $d = 180°$. In other words, the direction of motion in signal B was opposite to that of signal A. Error bars show ± 1 SE. The horizontal dashed line is a prediction for probability summation between independent mechanisms ($\beta = 4$ in the Quick pooling formula). This prediction provides a poor account of the data suggesting interactions between motion mechanisms.

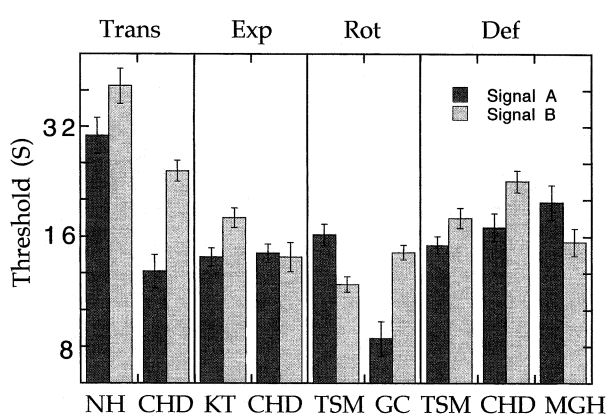

Fig. 6. Coherence thresholds (S = percentage of signal dots) for signals presented alone in Experiment 2 with $d = 180°$. Dark bars are for signal A and pale bars are for signal B. Stimulus conditions were interleaved within experimental sessions. Error bars show ± 1 SE.

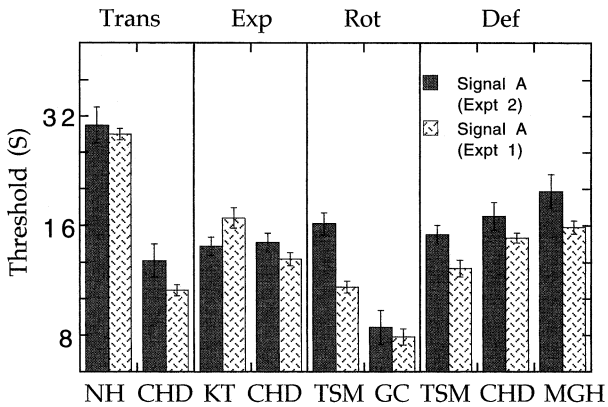

Fig. 7. Coherence thresholds (S = percentage of signal dots) for signal A when presented alone in Experiments 1 and 2. Solid bars are for Experiment 2 (they are the same data as in Fig. 6) and patterned bars are for Experiment 1, averaged across different conditions of d. The experimental conditions for the two data sets differed only in the dot directions for signal B for which thresholds were being tracked simultaneously with signal A. For the solid bars, the two signals had opposite directions of motion, whereas for the patterned bars, direction differences varied between 15 and 90°. Error bars show ± 1 SE.

We also reject the possibility that learning might have contaminated the results from Experiment 2. For CHD the deformation condition was the last stimulus condition to be performed whereas for TSM it was the first; nevertheless, both observers show the same trends.

The data in Fig. 5 prompt us to make several points but first it is important to appreciate the details of how our stimuli were constructed. Crucially, the average statistical distribution of dot velocities was the same for all of the complex motion stimuli and for noise. For example, all dot directions were equally likely. Furthermore, for all complex motion stimuli, the rate of change of local motion directions as a function of polar angle of nominal dot position was identical and smooth. Regardless of signal level then, the only difference between our complex motion stimuli was their spatial configuration. This means that a local analysis of motion over a small number of dots in one region of a complex motion stimulus is very similar to that in some other region of any other complex motion stimulus. This is true for comparisons amongst individual components and amongst compound stimuli. Thus, it is difficult to account for the different results in Experiment 2 in terms of either a local description of the stimulus or a local analysis by the visual system. A

more likely explanation is that these results reflect differences in global properties of the detecting mechanisms. This leads us to suggest that the characteristics of the detecting mechanisms for deformation are different from those for the other motion stimuli that we have investigated. We interpret this result as evidence for an inhibitory input to the deformation mechanism for stimuli in the mechanism's antipreferred direction (Meese & Harris, 1996), consistent with the second property of a complex motion extractor (Section 1). We report further evidence for this in Experiment 3.

First, however, we return to Fig. 6 which highlights the existence of asymmetries in sensitivity to opposite directions of motion (compare column pairs for each observer). Previous work (Edwards & Badcock, 1993) has found thresholds to be higher for expansion (signal A) than for contraction (signal B), though we did not find this here (see KT and CHD). Although the bases of the asymmetries in our data remain unclear, they do go to show the value of normalising the strengths of the component signals in the compound stimulus. Without this normalisation, a single component could have dominated the compound stimulus and the potential for observing summation would have been compromised.

It is of passing interest that the coherence thresholds for TSM and CHD in Fig. 6 are slightly higher than those that we have reported previously for the same observers and stimuli (Meese & Harris, under review). Further comparisons can be made in Fig. 7, where the filled bars are the same as those in Fig. 6 and the patterned bars are the average thresholds for signal A in Experiment 1. In eight out of nine cases, coherence thresholds were slightly lower in Experiment 1, even though signal A was identical in the two experiments. The only difference in experimental conditions was the dot directions for signal B, for which trials were interleaved with those of signal A. Specifically, in Experiment 1, signal B had directions between 0 and 90° relative to signal A, whereas in Experiment 2, the difference between the dot directions of signal A and B was 180°. In other words, performance was most degraded when the observer had to monitor motion directions of opposite sign. This is generally consistent with previous work, where reaction times (Ball & Sekuler, 1980) and contrast detection thresholds (Ball, Sekuler, & Machamer, 1983) for translating random-dot patterns were found to increase with an increase in the range of potential target directions. This decrease in sensitivity is often attributed to stimulus uncertainty (Ball & Sekuler, 1980; Graham, 1989).

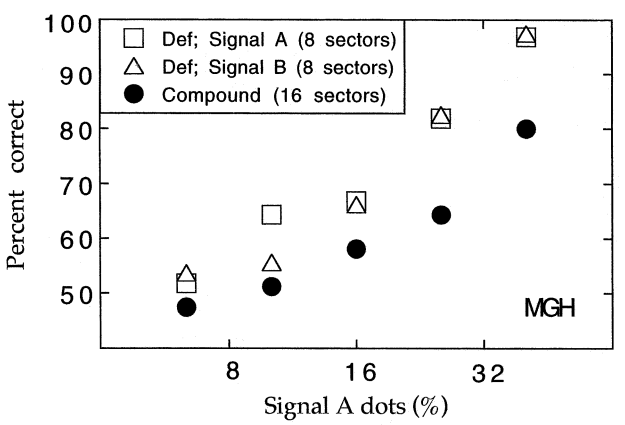

Fig. 8. Psychometric functions for detecting deformation components with opposite signs (open symbols) and a compound made from their superposition (filled symbols). Signal dots for components with opposite signs were contained in alternate sectors of the display.

3.4. Experiment 3: antagonism for deformation mechanisms

One problem with Experiment 2 is that signal dots travelling in opposite directions could annihilate each other, either physically in the display, or within early opponent motion mechanisms (e.g. Qian, Andersen, & Adelson, 1994). In Experiment 3 this problem was avoided by notionally dividing the display into 16 equally sized sectors and assigning signal dots of opposite sign to alternate sectors. Unlike in Experiments 1 and 2, no attempt was made to normalise sensitivity to the two components, and their weight in the compound stimulus was equal. Results are shown in Fig. 8 for a single observer MGH. The open symbols are the psychometric functions for the two component conditions and the filled symbols are for the compound condition. The psychometric function for the compound stimulus is shifted to the right indicating that the compound stimulus was more difficult to detect than either of the components, consistent with the deformation results from Experiment 2.

4. General discussion

4.1. Global or local mechanisms?

In recent years, research has moved on from understanding the properties of local mechanisms to address questions concerning global processes (e.g. Smith, Scott-Samuel, & Singh, 2000). In isolation, the results from Experiment 1 imply little about the properties of global complex motion processing. For example, it could be that detection is being mediated by lower order unidirectional motion units that perhaps pool over only a small region of the moving image. Such mechanisms may or may not feed into higher order complex motion mechanisms. However, earlier work by others and by us, indicates that observers enhance

performance by employing motion mechanisms that pool over different directions at different positions to perform detection of complex motion (Harris & Meese, 1996; Meese & Harris, under review) and discrimination of its direction (Morrone et al., 1995; Burr et al., 1998). For stimuli of the type used here, this pooling of structured motion is often close to linear and always greater than quadratic, and results in coherence thresholds close to those found in the present study (e.g. Fig. 7). As the complex motion stimuli used in the present study were the same as those we have used previously, the most reasonable interpretation of the present data is that they reflect the characteristics of these global pooling mechanisms.

4.2. Related work

Several previous studies suggest psychophysical mechanisms for detecting complex motion. Here we have used a subthreshold summation technique and random dot stimuli to show that these mechanisms are broadly tuned for direction (probably somewhere between ± 35 and $\pm 60°$, depending upon their sampling density). This result is generally consistent with Snowden and Milne's (1996) adaptation study, where mechanism bandwidth (half-width at half-height) for expansion, rotation and spiral detecting mechanisms were estimated at 47°. The present study, however, requires no assumptions about adaptation; a process that in spatial vision now appears more complicated (Wilson & Humanski, 1993; Foley & Chen, 1997) than was often assumed.

Other studies have also reported broad direction tuning for unidirectional motion mechanisms. For example, Ball and Sekuler (1979) used translating random dot stimuli in the presence of forward noise-masks. They found reaction times to be half of their maximum when dot directions about 50° either side of the test stimulus were removed from the mask. A similar breadth of psychophysical effect was found by Levinson and Sekuler (1980) who used an adaptation paradigm and measured contrast detection thresholds for translating random dot patterns using a method of adjustment. Raymond (1993) performed a similar experiment using coherence thresholds and estimated direction bandwidths to be between ± 35 and $\pm 40°$. Anderson, Burr and Morrone (1991) used spatially jittering masks with variable orientation and measured contrast thresholds for identifying the direction (left versus right) of drifting gratings. The bandwidth of threshold elevation was $\pm 40°$ when the test spatial frequency was 0.1 cpd and $\pm 24°$ when the test spatial frequency was 10 cpd. Georgeson and Scott-Samual (2000) estimated orientation bandwidths of motion mechanisms using a stimulus with interleaved frames of a grating and plaid whose component orientations θ, were manipulated relative to the vertical orientation of the grating. Georgeson and Scott-Samual's (2000) Gaussian derivative model suggested tuning functions that had a bandwidth of ± 45 to $\pm 60°$. In the last two studies, however, it is not clear whether the estimates of bandwidth represent estimates of direction bandwidth or orientation bandwidth, which single-cell work has shown can be different (Albright, 1984). In all of the above studies of unidirectional motion mechanisms, the estimates of mechanism bandwidth were based upon the bandwidth of a psychophysical function (e.g. threshold elevation), and no modelling was performed to take into account the possible effects of probability summation amongst multiple mechanisms (Graham, 1989) nor cross-orientation inhibition (e.g. Foley, 1994), which in some cases might be important. Nevertheless, these estimates are remarkably similar to the average direction half-width of cells in monkey MT which Rodman and Albright (1987) report as $\pm 44°$.

Our data do not allow us to see the details of how complex motion mechanisms are constructed, but one possibility is that appropriately positioned unidirectional motion mechanisms with appropriately broad direction tuning might feed into higher order summing units. Note that in this case, the direction bandwidths of the global mechanisms are determined entirely by the direction bandwidths of the unidirectional subunits. This possibility is fairly consistent with the evidence reviewed above and the eight-mechanism model in Fig. 4B. Another possibility is that bandwidths for complex motion mechanisms could be made broader by summing several subunits with overlapping receptive fields and neighbouring preferred directions. Given that most estimates of direction bandwidths for unidirectional motion mechanisms are narrower than $\pm 60°$, this kind of connectivity presumably would be required for a complex motion extractor (Zhang et al., 1993).

4.3. Inhibitory input?

One intriguing aspect of our data is the difference in results for deformation and the other complex motions in Experiment 2. As mentioned in the previous section, we interpret this as evidence for inhibitory input in the detecting mechanism's antipreferred directions for deformation, but no such input for the other mechanisms we have investigated. First we consider the consequence of having no inhibitory input.

In principle, a complex motion mechanism could be constructed from a template of unidirectional motion mechanisms matched to the appropriate pattern of complex motion. For example, if the template were for expansion, then the mechanism would respond to expansion, but also, for example, translation, because regardless of the direction of translation the stimulus would coincide with one or more of the mechanism's

excitatory subunits. The same point can be made for rotation, spiral and translation mechanisms. Thus, if mechanisms of this type are used by vision, then the implication is that they must be involved in a population code where stimulus properties are deduced from the distribution of activity across multiple mechanisms selective for different patterns of motion. One widely discussed possibility is that mechanisms of this kind might be involved in navigation (e.g. Tanaka & Saito, 1989; Graziano, Andersen, & Snowden, 1994; Duffy & Wurtz, 1995).

In contrast, the broad direction tuning and inhibitory input implied for the deformation mechanism are consistent with two of the properties required for extracting the deformation component from the retinal flow field (Zhang et al., 1993). Intuitively, the purpose of these two properties is as follows. Cosine direction tuning means that only the local motion vector parallel to the preferred direction of the local subunit is encoded, essentially achieving vector decomposition. The extension of this property to include a negative inhibitory lobe means that the mechanism would not respond to uniform translation (or any other component of optic flow). This is because the contribution of every subunit that is excited by the translating stimulus would be nullified by another subunit with opposite preferred direction and matched level of inhibition. A mechanism with these types of analytic properties would be useful in computing the tilt and slant of surfaces relative to an observer (Koenderink, 1986; Meese, Harris, & Freeman, 1995; Meese & Harris, 1997; Xiao, Marcar, Raiguel, & Orban, 1997; Freeman & Fowler, 2000).

Finally, we note that psychophysics (Burr et al., 1998) and neurophysiology (see Orban, 1997 for a review) suggest that receptive fields can be large for expansion and rotation mechanisms (around 80°). While these properties might be helpful for the needs of navigation, the generally smaller sizes and multiple instances of planar surfaces in a visual environment (e.g. an office) suggest that mechanisms for calculating surface slant should include those with much smaller receptive fields. This issue remains to be addressed.

Acknowledgements

Some of this work has previously been presented in abstract form (Meese & Harris, 1996; Meese, 2000; Meese et al., 2000).

Appendix A

Here we first describe the '2-mechanism model' shown in Figs. 2 and 3. The model is so called because only two mechanisms contribute to detection. Conceptually, however, these two mechanisms come from a larger set of four cardinal mechanisms. Indeed, in Fig. 4 where larger numbers of more closely spaced mechanisms are considered, it is more natural to refer to the total number of mechanisms in the model, regardless of how many of them respond to the stimuli. For this reason, the same model (though with different estimates of mechanism gain) is referred to as a '2-mechanism model' in Figs. 2 and 3 and as a '4-mechanism model' in Fig. 4.

A.1. 2-Mechanism model

The model details are the same regardless of the stimulus and mechanism type. We assume one detecting mechanism whose preferred stimulus is signal A and another whose preferred stimulus is signal B when $d = 90°$.
Let:

δ_i	the preferred dot 'directions' of the i-th mechanism (Fig. 1) ($\delta_1 = 0°$; $\delta_2 = 90°$)
d_j	the dot 'directions' of the j-th signal (Fig. 1) ($j = \mathrm{A}, \mathrm{B}$)
α_i	mechanism gain ($i = 1, 2$)
$S_{j(\mathrm{cmpnd})}$	proportion of signal j dots in the compound stimulus [A + B]
S_j	proportion of signal j dots in the component stimuli [A or B]
$S_\mathrm{A}/S_{\mathrm{A(cmpnd)}} = S_\mathrm{B}/S_{\mathrm{B(cmpnd)}}$	summation index (SI)

Thus:

$$S_{\mathrm{A(cmpnd)}} = S_{\mathrm{B(cmpnd)}}\, S_\mathrm{A}/S_\mathrm{B}. \tag{1}$$

Estimates of mechanism gains are given by:

$$\alpha'_1 = 1/S_\mathrm{A}, \tag{2}$$

and

$$\alpha'_2 = 1/S_{\mathrm{B90}}, \tag{3}$$

at coherence threshold, where S_{B90} was measured in the condition where $d_\mathrm{B} = 90°$. Multiplying each side of Eq. (2) by each side of Eq. (1), respectively, and rearranging, usefully gives:

$$\alpha'_1 = S_{\mathrm{B(cmpnd)}}/(S_{\mathrm{A(cmpnd)}}\, S_\mathrm{B}). \tag{4}$$

Using the Quick pooling formula for detection (Quick, 1974; Graham, 1989), the total response at coherence (detection) threshold is given by:

$$\mathrm{RESP}_\mathrm{TOT} = \left(\sum_i [\mathrm{RESP}_i^\beta]\right)^{1/\beta} = 1, \tag{5}$$

where RESP_i is the response of the i-th mechanism, given by:

$$\mathrm{RESP}_i = \alpha_i \sum_j (S_j \ \mathrm{SENS}_{ij}), \tag{6}$$

where SENS_{ij} is the sensitivity of the i-th mechanism to the j-th signal. The mechanisms have cosine direction tuning functions and so SENS_{ij} is given by:

$$\mathrm{SENS}_{ij} = \cos(\mathrm{diff}_{ij}), \tag{7}$$

where diff_{ij} is given by:

$$\mathrm{diff}_{ij} = \delta_j - d_i; \quad \text{if } |\mathrm{diff}_{ij}| > 90 \quad \text{then } \mathrm{diff}_{ij} = 0.$$

Note, for the mechanisms modelled here, no inhibitory inputs are considered. The results of Experiments 2 and 3 suggest that the deformation mechanism does have inhibitory input, in which case, for that stimulus, Eq. (7) should be: $\mathrm{SENS}_{ij} = \cos(\delta_j - d_i)$. This is immaterial for the model predictions in Figs. 2 and 3 and would have the effect of decreasing the predicted level of summation for some of the models in Fig. 4.

Restricting $\delta_j - d_i \leq 90°$, expanding Eq. (5) and using the empirical estimates of mechanism gain, for the compound stimulus we have:

$$1 = \{[\alpha'_1(S_{\mathrm{A(cmpnd)}} + S_{\mathrm{B(cmpnd)}} \cos(d_\mathrm{B}))]^\beta + [\alpha'_2 \, S_{\mathrm{B(cmpnd)}} \sin(d_\mathrm{B})]^\beta\}.$$

Factorising and substituting Eqs. (3) and (4) gives:

$$1 = \{(S_{\mathrm{B(cmpnd)}}/S_\mathrm{B})^\beta \, [1 + (S_{\mathrm{B(cmpnd)}}/S_{\mathrm{A(cmpnd)}}) \cos(d_\mathrm{B})]^\beta + [(S_{\mathrm{B(cmpnd)}}/S_{\mathrm{B90}}) \sin(d_\mathrm{B})]^\beta\}.$$

Factorising again gives:

$$1 = (S_{\mathrm{B(cmpnd)}}/S_\mathrm{B})^\beta \times \{[1 + (S_\mathrm{B}/S_\mathrm{A}) \cos(d_\mathrm{B})]^\beta + [(S_\mathrm{B}/S_{\mathrm{B90}}) \sin(d_\mathrm{B})]^\beta\}.$$

Finally, this rearranges to give a prediction for the summation index,

$$\mathrm{SI}_{[\text{2cosine mechs}]} = \{[1 + (S_\mathrm{B}/S_\mathrm{A}) \cos(d_\mathrm{B})]^\beta + [(S_\mathrm{B}/S_{\mathrm{B90}}) \sin(d_\mathrm{B})]^\beta\}^{1/\beta}. \tag{8}$$

The parameter β is the only free parameter. It is the summation exponent in the Quick pooling formula and was set to four as is commonly done to simulate the effects of probability summation (e.g. Graham, 1989; Meese & Williams, 2000).

A.2. 1-Mechanism model

In the case of the '1-mechanism model', it was assumed that for the compound stimulus, the mechanism tuned to 90° was ignored, simplifying Eq. (8) to:

$$\mathrm{SI}_{[\text{1 cosine mechs}]} = [1 + (S_\mathrm{B}/S_\mathrm{A}) \cos(d_\mathrm{B})], \tag{9}$$

which has no free parameters.

Note that the model predictions shown in Figs. 2 and 3 do not produce smooth curves, but tend to kink due to the empirical $(S_\mathrm{B}/S_\mathrm{A})$ term for which there was an independent estimate for each value of d_B (denoted d in the figures).

Appendix B

Here we describe the models shown in Fig. 4. We make the simplifying assumption that all mechanisms have equal gain, so α_i is replaced by α. The relative weight (w) of the two signals in the compound stimulus is determined by the sensitivities to the two signals alone, in the same way as was done in the experiments.

The aim of the analysis was to show how model predictions vary depending on the bandwidths and placement of the detecting mechanisms.

At coherence threshold, combining Eq. (5) and Eq. (6) gives the general case:

$$1 = \alpha^\beta \sum_i \left\{ \left[\sum_j (S_j \ \mathrm{SENS}_{ij}) \right]^\beta \right\}. \tag{10}$$

Letting

$$S_\mathrm{B} = w S_\mathrm{A}, \tag{11}$$

and combining Eq. (10) and Eq. (11), coherence threshold for signal A in the compound stimulus is given by:

$$S_{\mathrm{A(cmpnd)}} = \left\{ \sum_i [(\mathrm{SENS}_{i\mathrm{A}} + w \ \mathrm{SENS}_{i\mathrm{B}})^\beta] \right\}^{(-1/\beta)} \Big/ \alpha, \tag{12}$$

and the coherence threshold for a signal A when presented alone is given by:

$$S_\mathrm{A} = \left[\sum_i (\mathrm{SENS}_{i\mathrm{A}}^\beta) \right]^{(-1/\beta)} \Big/ \alpha. \tag{13}$$

The summation index is derived by dividing Eq. (13) by Eq. (12), to give:

$$\mathrm{SI}_{[\text{many mechs}]} = \left[\sum_i (\mathrm{SENS}_{i\mathrm{A}}^\beta) \right]^{(-1/\beta)} \cdot \left\{ \sum_i [(\mathrm{SENS}_{i\mathrm{A}} + w \ \mathrm{SENS}_{i\mathrm{B}})^\beta] \right\}^{1/\beta},$$

where, from Eq. (11), the weight w is given by dividing the proportion of signal dots at threshold for each of the two signals when presented alone:

$$w = \left[\sum_i (\mathrm{SENS}_{i\mathrm{B}}^\beta) \right]^{(-1/\beta)} \cdot \left[\sum_i (\mathrm{SENS}_{i\mathrm{A}}^\beta) \right]^{(1/\beta)}.$$

Mechanism tuning functions were either cosine ($\mathrm{SENS}_{ij} = \cos[\mathrm{diff}]$), as in Eq. (7) of Appendix A, or Gaussian ($\mathrm{SENS}_{ij} = G[\delta_j, d_i, \sigma]$), where $G[\delta_j, d_i, \sigma]$ is given by:

$$G[\delta_j, d_i, \sigma] = \exp[-(\mathrm{diff}g)^2/(2\sigma^2)],$$

where σ is a spread parameter (half-width at half-height $= 1.18\sigma$) and diff$g$ is given by:

$$\mathrm{diff}g = (\delta_j - d_i);$$

$$\text{IF } |\mathrm{diff}g| > 180 \quad \text{THEN } \mathrm{diff}g = (\delta_j - d_i) - 360.$$

We have not attempted to model the possible effects of spatial probability summation. In the spatial domain this is important for estimates of bandwidth (e.g. Bergen, Wilson, & Cowan, 1979; Graham, 1989) because of the phase selectivity of the detecting mechanisms. If it were the case, however, that for each type of mechanism that contributes significantly to detection, the relative sensitivities to signal A and B (with d fixed) were the same regardless of its position, then spatial probability summation is unimportant. This is a reasonable assumption for the stimuli and detecting mechanisms considered here.

Appendix C

Here, we explain why the issues raised in the Introduction concerning template matching and one- and two-dimensional mechanisms, have no bearing on the models presented in this paper. Suppose that the deformation stimulus used as signal A in Experiment 1 (Fig. 1D) is detected by a pair of orthogonal one-dimensional shear mechanisms (ie. vertical and horizontal shear mechanisms). Both mechanisms would respond equally when signal A is deformation. Both mechanisms would also respond equally when signal B is deformation, and their responses would decrease equally as d is increased. Thus, because the responses of the two mechanisms are matched for all of the stimuli in our summation experiments (e.g. Fig. 1D) they can be treated as a single mechanism in the summation model (even though their directional templates are orthogonal) (Robson & Graham, 1981). Thus, it is immaterial to the issues examined in this paper whether there is a single two-dimensional mechanism or a pair of orthogonal one-dimensional mechanisms.

References

Albright, T. D. (1984). Direction and orientation selectivity of neurons in visual area MT of the macaque. *Journal of Neurophysiology*, *52*, 1106–1130.

Allman, J., Miezin, F., & McGuiness, E. (1985). Direction- and velocity-specific responses from beyond the classical receptive field in the middle temporal visual area (MT). *Perception*, *14*, 105–126.

Anderson, S. J., Burr, D. C., & Morrone, M. C. (1991). Two dimensional spatial and spatial-frequency selectivity of motion-sensitive mechanisms in human vision. *Journal of the Optical Society of America A*, *8*, 1340–1351.

Ball, K., & Sekuler, R. (1979). Masking of motion by broadband and filtered directional noise. *Perception and Psychophysics*, *26*, 206–214.

Ball, K., & Sekuler, R. (1980). Models of stimulus uncertainty in motion perception. *Psychological Review*, *87*, 435–469.

Ball, K., Sekuler, R., & Machamer, J. (1983). Detection and identification of moving targets. *Vision Research*, *23*, 229–238.

Bergen, J. R., Wilson, H. R., & Cowan, J. D. (1979). Further evidence for four mechanisms mediating vision at threshold: sensitivities to complex gratings and aperiodic stimuli. *Journal of the Optical Society of America*, *A69*, 1580–1587.

Bex, P. J., Metha, A. B., & Makous, W. (1998). Psychophysical evidence for a functional hierarchy of motion processing mechanisms. *Journal of the Optical Society of America*, *A15*, 769–776.

Bex, P. J., Metha, A. B., & Makous, W. (1999). Enhanced motion aftereffect for complex motions. *Vision Research*, *39*, 2229–2238.

Burr, D. C., Morrone, M. C., & Vaina, L. M. (1998). Large receptive fields for optic flow detection in humans. *Vision Research*, *38*, 1731–1743.

Cornsweet, T. N. (1962). The staircase-method in psychophysics. *American Journal of Psychology*, *75*, 485–491.

DeBruyn, B., & Orban, G. A. (1990). The role of direction information in the perception of geometric optic flow components. *Perception and Psychophysics*, *47*, 433–438.

Duffy, C. J., & Wurtz, R. H. (1995). Response of monkey MST neurons to optic flow stimuli with shifted centres of motion. *Journal of Neuroscience*, *15*, 5192–5208.

Edwards, M., & Badcock, D. R. (1993). Asymmetries in the sensitivity to motion in depth: a centripetal bias. *Perception*, *22*, 1013–1023.

Finney, D. J. (1971). *Probit Analysis* (3). London: Cambridge University Press.

Foley, J. M. (1994). Human luminance pattern vision mechanisms: masking experiments require a new model. *Journal of the Optical Society of America A*, *11*, 1170–1719.

Foley, J. M., & Chen, C.-C. (1997). Analysis of the effect of pattern adaptation on pattern pedestal effects: a two-process model. *Vision Research*, *37*, 2779–2788.

Freeman, T. C. A., & Fowler, T. A. (2000). Unequal retinal and extra-retinal motion signals produce different perceived slants of moving surfaces. *Vision Research*, *40*, 1857–1868.

Freeman, T. C. A., & Harris, M. G. (1992). Human sensitivity to expanding and rotating motion: effects of complementary masking and directional structure. *Vision Research*, *32*, 81–87.

Georgeson, M. A., Freeman, T. C. A., & Scott-Samuel, N. E. (1996). Sub-pixel accuracy: psychophysical validation of an algorithm for fine positioning and movement of dots on visual displays. *Vision Research*, *36*, 605–612.

Graham, N. (1989). *Visual Pattern Analyzers*. Oxford: Oxford University Press.

Graziano, M. S. A., Andersen, R. A., & Snowden, R. J. (1994). Tuning of MST neurons to spiral motions. *The Journal of Neuroscience*, *14*, 54–67.

Gurney, K., & Wright, M. J. (1996). Rotation and radial motion thresholds support a two-stage model of differential-motion analysis. *Perception*, *25*, 5–26.

Harris, M. G., & Meese, T. S. (1996). Human vision employs pooling mechanisms for rotation, expansion and deformation components of optic flow. *Perception*, *25*(Suppl.), 129.

Ivins, J., Porrill, J, Frisby, J., & Orban, G. (1999). The 'ecological' probability density function for linear optic flow: implications for neurophysiology. *Perception*, *28*, 17–32.

Koenderink, J. J. (1986). Optic flow. *Vision Research*, *26*, 161–179.

Levinson, E., & Sekuler, R. (1980). A two-dimensional analysis of direction-specific adaptation. *Vision Research*, *20*, 103–107.

McKee, S. P., Klein, S. A., & Teller, D. Y. (1985). Statistical properties of forced-choice psychometric functions: implications of probit analysis. *Perception and Psychophysics*, *37*, 286–298.

Meese, T. S. (1995). Using the standard staircase to measure the point of subjective equality: a guide based on computer simulations. *Perception and Psychophysics*, *57*, 267–281.

Meese, T. S. (2000). Complex motion detection in human vision. *Spatial Vision*, *14*, 91–92.

Meese, T. S., Cooper, G., & Hunjan, N. (2000). Broad direction tuning for complex motion detectors [ARVO abstract]. *Investigative Ophthalmology and Visual Science*, *41*(4), S721.

Meese, T. S., Harris, M. G., & Freeman, T. C. A. (1995). Speed gradients and the perception of surface slant: analysis is two dimensional not one dimensional. *Vision Research*, *35*, 2879–2888.

Meese, T. S., & Harris, M. G. (1996). Deformation extractors in human vision: evidence from subthreshold summation experiments. *Perception*, *25*(Suppl.), 129–130.

Meese, T. S., & Harris, M. G. (1997). Computation of surface slant from optic flow: orthogonal components of speed gradient can be combined. *Vision Research*, *37*, 2369–2379.

Meese, T. S., Harris, M. G. (under review). Independent detectors for orthogonal components of complex motion, *Perception*.

Meese, T. S., & Williams, C. B. (2000). Probability summation for multiple patches of luminance modulation. *Vision Research*, *40*, 2101–2113.

Morgan, M. J., & Aiba, T. A. (1985). Vernier acuity predicted from changes in the light distribution of the retinal image. *Spatial Vision*, *1*, 151–161.

Morrone, M. C., Burr, D. C., & DiPietro, S. (1999). Cardinal directions for optic flow. *Current Biology*, *9*, 763–766.

Morrone, M. C., Burr, D. C., & Vaina, L. M. (1995). Two stages of visual processing for radial and circular motion. *Nature*, *376*, 507–509.

Orban, G. A. (1997). Visual processing in macaque area MT/VS and its satellites (MST and MSTV). In K. S. Rockland, J. H. Kaas, & A. Peters (Eds), *Cerebral Cortex V12*. London: Plenum Press.

Qian, N., Andersen, R. A., & Adelson, E. H. (1994). Transparent motion perception as detection of unbalanced motion signals. I. Psychophysics. *The Journal of Neuroscience*, *14*, 7357–7366.

Quick, R. F. (1974). A vector-magnitude model of contrast detection. *Kybernetik*, *16*, 65–67.

Raymond, J. E. (1993). Movement direction analyzers: independence and bandwidth. *Vision Research*, *33*, 767–775.

Regan, D., & Beverley, K. I. (1978). Looming detectors in the human visual pathway. *Vision Research*, *18*, 415–421.

Robson, J. G., & Graham, N. (1981). Probability summation and regional variation in contrast sensitivity across the visual field. *Vision Research*, *21*, 409–418.

Rodman, H. R., & Albright, T. D. (1987). Coding of visual stimulus velocity in area MT of the macaque. *Vision Research*, *27*, 2035–2048.

Sekuler, A. B. (1992). Simple-pooling of unidirectional motion predicts speed discrimination for looming stimuli. *Vision Research*, *32*, 2277–2288.

Smith, A. T., Scott-Samuel, N. E., & Singh, K. D. (2000). Global motion adaptation. *Vision Research*, *40*, 1069–1075.

Snowden, R. J., & Milne, A. B. (1996). The effects of adapting to complex motions: position invariance and tuning to spiral motions. *Journal of Cognitive Neuroscience*, *8*, 435–452.

Tanaka, K., & Saito, H.-A. (1989). Analysis of the visual field by direction, expansion/contraction, and rotation cells clustered in the dorsal part of the medial superior temporal area of the macaque monkey. *Journal of Neurophysiology*, *62*, 626–641.

Watson, A. B. (1982). Summation of grating patches indicates many types of detector at one retinal location. *Vision Research*, *22*, 17–25.

Wetherill, G. B., & Levitt, H. (1965). Sequential estimation of points on a psychometric function. *British Journal of Mathematical and Statistical Psychology*, *18*, 1–10.

Wilson, H. R., & Humanski, R. (1993). Spatial frequency adaptation and contrast gain control. *Vision Research*, *33*, 1133–1149.

Xiao, D.-K., Marcar, V. L., Raiguel, S. E., & Orban, G. A. (1997). Selectivity of macaque MT/V5 neurons for surface orientation in depth specified by motion. *European Journal of Neuroscience*, *9*, 956–964.

Zhang, K., Sereno, M. I., & Sereno, M. E. (1993). Emergence of position-independent detectors of sense of rotation and dilation with Hebbian learning: an analysis. *Neural Computation*, *5*, 597–612.